ARTICLE
Journal of Cellular Biochemistry 108:1132–1142 (2009)

Journal of Cellular Biochemistry

Purification and Characterization of Heparan Sulfate From Human Primary Osteoblasts

Sadasivam Murali,[1] Kerry J. Manton,[1] Vinalia Tjong,[2] Xiaodi Su,[2] Larisa M. Haupt,[1] Simon M. Cool,[1,3] and Victor Nurcombe[1*]

[1] *Stem Cells and Tissue Repair Group, Institute of Medical Biology, A*STAR (Agency for Science, Technology and Research), 8A Biomedical Grove, #06-06 Immunos, Singapore 138648, Singapore*

[2] *Micro- & Nano-Systems Cluster, Institute of Materials Research and Engineering, Singapore 117602, Singapore*

[3] *Department of Orthopaedic Surgery, Yong Loo Lin School of Medicine, National University of Singapore, Singapore 119074, Singapore*

ABSTRACT

Heparan sulfate (HS) is a linear, highly variable, highly sulfated glycosaminoglycan sugar whose biological activity largely depends on internal sulfated domains that mediate specific binding to an extensive range of proteins. In this study we employed anion exchange chromatography, molecular sieving and enzymatic cleavage on HS fractions purified from three compartments of cultured osteoblasts—soluble conditioned media, cell surface, and extracellular matrix (ECM). We demonstrate that the composition of HS chains purified from the different compartments is structurally non-identical by a number of parameters, and that these differences have significant ramifications for their ligand-binding properties. The HS chains purified of conditioned medium had twice the binding affinity for FGF2 when compared with either cell surface or ECM HS. In contrast, similar binding of BMP2 to the three types of HS was observed. These results suggest that different biological compartments of cultured cells have structurally and functionally distinct HS species that help to modulate the flow of HS-dependent factors between the ECM and the cell surface. J. Cell. Biochem. 108: 1132–1142, 2009.

KEY WORDS: GLYCOSAMINOGLYCANS; EXTRACELLULAR MATRIX; GROWTH FACTORS; BONE; DIFFERENTIATION

Heparan sulfate proteoglycans (HSPGs) are expressed in the pericellular space as either transmembrane (primarily the syndecans) or glycosylphosphotidylinositol-linked forms (the glypicans) or, alternatively, they can be directly secreted into, and incorporated by the extracellular matrix (such as for the perlecans) [Iozzo, 2001]. Generic HSPG structure consists of a core protein to which one or more linear glycosaminoglycan (GAGs) chains are attached at specific serine–glycine residues. Heparan sulfates (HSs) have complex sulfated domain structures, that are initially synthesized as non-sulfated polysaccharides of D-glucuronic acid-*N*-acetyl-D-glucosamine (GlcA-GlcNAc) repeats [Casu and Lindahl, 2001; Esko and Lindahl, 2001; Esko and Selleck, 2002; Lindahl et al., 1998]. Concurrent with polymerization of the HS chain, a series of enzymatic modifications occur that generate diverse sulfated domains at intervals along a growing chain.

The non-sulfated precursor disaccharide units are first modified by coordinated *N*-deacetylation and *N*-sulfation of GlcNAc residues by *N*-deacetylase/*N*-sulfotransferase enzymes, so forming *N*-sulfoglucosamine (GlcNS). The *N*-sulfated polymer then undergoes a further series of modifications: C5-epimerization of GlcA to iduronic acid (IdoA), *O*-sulfation at the C2 of IdoA by 2-*O*-sulfotransferase, at the C6 of GlcNS or GlcNAc by 6-*O*-sulfotransferase, and at the C3 of GlcN by 3-*O*-sulfotransferase [Murphy et al., 2004; Wei et al., 2005]. The high degree of structural diversity observed in HS chains is believed to be important for the functional specificity of these macromolecules [Zako et al., 2003].

Abbreviations used: ECM, extracellular matrix; GAGs, glycosaminoglycans; HS, heparan sulfate; HSPGs, heparan sulfate proteoglycans; HS2OST1, heparan sulfate 2-*O*-sulfotransferase 1; HS6ST1, heparan sulfate 6-*O*-sulfotransferase 1; HS6ST2, heparan sulfate 6-*O*-sulfotransferase 2; HS6ST3, heparan sulfate 6-*O*-sulfotransferase 3; NDST-1, *N*-deacetylase/*N*-sulfotransferase 1; NDST-2, *N*-deacetylase/*N*-sulfotransferase 2; NDST-3, *N*-deacetylase/*N*-sulfotransferase 3; NDST-4, *N*-deacetylase/*N*-sulfotransferase 4; TGAGs, total glycosaminoglycans.

Grant sponsor: Singapore's Agency for Science Technology and Research (A-STAR); Grant sponsor: Institute of Medical Biology, Singapore.

*Correspondence to: Dr. Victor Nurcombe, 8A Biomedical Grove, #06-06 Immunos, Singapore 138648, Singapore. E-mail: victor.nurcombe@imb.a-star.edu.sg

Received 7 July 2009; Accepted 11 August 2009 • DOI 10.1002/jcb.22340 • © 2009 Wiley-Liss, Inc.

Published online 23 September 2009 in Wiley InterScience (www.interscience.wiley.com).

The unsulfated GlcA-(1(4)-GlcNAc disaccharide sequence is the most common in HS; such sequences demarcate the regions of sulfated domain, wherein segregated blocks of repeating GlcA-(1 → 4)-GlcNAc disaccharides (*N*-acetyl (NA) domains) and blocks of highly sulfated, heparin-like IdoA-(1 → 4)-GlcNS disaccharides (*N*-sulfate (NS)) domains are interspersed. The NA and NS domains are separated by NA/NS transition segments that consist of both GlcNAc- and GlcNS-containing disaccharides [Murphy et al., 2004]. The non-template-driven diversity of HS structure thus is able to give rise to a wide range of biological functions.

Several studies have demonstrated that the binding of growth factors to HS (and the resultant mitogenic activity) happens only when specific structural features are present within the HS chain [Walker et al., 1994]. Such features include sulfation at specific positions within a disaccharide; 6-*O*-sulfated *N*-sulfate glucosamine and 2-*O*-sulfated iduronic acid residues are particularly important, and minimum binding sequences are generally at least five to six disaccharides in length [Pye and Gallagher, 1999; Lyon et al., 2000; Ostrovsky et al., 2002]. The precise structure of HS that is involved in these interactions remains elusive, but their differential partitioning, either shed or secreted into the soluble compartment, on the cell surface, or fixed into the ECM suggests that the structures may be specific to their location [Ashikari-Hada et al., 2004; Whitelock and Iozzo, 2005].

Given their intrinsic complexity, comparative structural and functional analyses of HS chains isolated from the medium, cell surface and ECM from the same cultured cell type should yield important information to help explain how cells manage the extremely rich flow of sugar-dependent signaling during cell growth and differentiation. In the present study, we focus on the comparative structural characterization and functional analyses of HS chains purified simultaneously from the three compartments of cultured human osteoblasts. We show that the structural differences in HS variants relates to their ligand-binding functions.

MATERIALS AND METHODS

MATERIALS

Heparinase, Heparitnase I and II, chondroitin ABC lyase and unsaturated HS disaccharides standards were obtained from Seikagaku Kogyo Co. (Tokyo). Bio-Gel P2, P6 and UNO Q-Sphere were from BioRad Laboratories (Hercules, CA). Sepharose CL-6B was supplied from Pharmacia Biotech Inc. (Uppsala, Sweden). Amicon Ultra-15 centrifugal filter devices were supplied by Millipore (Billerica, MA). Pronase and neuraminidase were purchased from Sigma–Aldrich (St. Louis, MO).

CULTURE OF PRIMARY HUMAN OSTEOBLASTS

Human osteoblasts cultures were derived from explants of calvarial bone obtained from a 19-year-old male donor after appropriate consent and with strict adherence to the ethical guidelines of the Biomedical Research Council of Singapore and the National University Hospital, Singapore. Briefly, the bone tissue was freed of any muscle or other connective tissue and macro-dissected into 2 cm^2 pieces. The bone chips were then seeded in 154 cm^2 Petri dishes in 25 ml of maintenance media (DMEM, 4,500 mg/L glucose supplemented with 10% FCS, 2 mM L-glutamine, 25 μg/ml L-ascorbic-2-phosphate, 100 U/ml penicillin–streptomycin sulfate and 100 μg/ml Fungizone). The cultures were left undisturbed for 1 week following initial plating, and the media changed every 5 days until confluent, at which stage cells were passaged with 0.125% trypsin. All experiments and HSPG extractions were performed in triplicate with passage 2 or 3 cultures.

EXTRACTION OF PROTEOGLYCOSAMINOGLYCANS (PGAGs) FROM HUMAN OSTEOBLASTS

The medium was gently removed from the flask without disturbing the cells and spun at 15,000*g* for 15 min to remove any cell debris, filtered a through 0.45 μm filter and stored at −20°C until required. The cells were washed with PBS and 10 ml of trypsin–EDTA added to the flask and incubated at 37°C for 25 min. The resulting cell/trypsin–EDTA solution was boiled for 10 min to deactivate the trypsin. The cell lysate was collected and spun at 15,000*g* for 15 min. The supernatant was collected, filtered through 0.45 μm filter and stored at −20°C until required. Then 10 ml of 6 M urea, 1% Triton X-100 solution (6 M urea in 0.1 M Tris–HCl, pH 7.4) was added for 5 min. The flask was scraped using rubber policeman and all materials collected, centrifuged, the supernatant collected, filtered through a 0.45 μm filter and stored at −20°C until required.

PURIFICATION OF TOTAL GLYCOSAMINOGLYCANS (TGAG)

The cell culture medium was subjected to ion-exchange chromatography on a UNO Q-Sphere column (15-ml) equilibrated in 50 mM Tris–HCl with 150 mM NaCl, pH 7.4 (low salt buffer) using a low-pressure liquid chromatography (Biologic-Duoflow chromatography system from Bio-Rad). The medium was loaded at a flow rate of 2 ml/min and the column washed with the same buffer until the baseline reach to zero. The bound material was eluted with a linear gradient of 1 M NaCl (high salt buffer). The peak fractions were pooled, concentrated and desalted with low salt buffer using an Amicon centrifugal filter (as per manufacturer's instructions) having a molecular mass cutoff of 5 kDa. The samples were quantified for the uronic acid content by the carbazole method [Berry et al., 2004] and stored at −20°C. Although the cell lysate was subjected to ion-exchange chromatography (as for the conditioned medium sample), the matrix samples were subjected to ion-exchange chromatography on a UNO Q-Sphere column (15-ml) equilibrated in 6 M urea in 0.1 M Tris–HCl, pH 7.4 with 1% Triton X-100 and 150 mM NaCl. The bound ECM material was eluted with a linear gradient of 1 M NaCl.

ISOLATION OF HS GAGs FROM HUMAN OSTEOBLASTS

The concentrated TGAG samples were treated with neuraminidase (0.1 U) for 4 h. Five volumes of 100 mM Tris acetate, pH 8.0, were then added to the sample which was further digested with chondroitinase ABC lyases (0.1 U) for 4 h at 37°C and further digested overnight with an equal volume of fresh enzyme. Finally, the core protein and the lyases were digested away with pronase (1/5 total volume of 10 mg/ml pronase in 500 mM Tris acetate, 50 mM calcium acetate, pH 8.0) at 37°C for 24 h. The entire mixture was then diluted 1:10 with low salt buffer, passed through a 15-ml UNO Q-Sphere column and eluted as described previously. The peak fractions were pooled, concentrated and desalted with water using

an Amicon centrifugal filter with mass cutoff of 5 kDa. The samples were quantified for the uronic acid content by carbazole method [Berry et al., 2004] and stored at −20°C.

ALKALI/BOROHYDRIDE ELIMINATIVE CLEAVAGE

The concentrated HS GAGs were treated with 1 M sodium borohydride under mild alkaline conditions (0.5 M NaOH for 16 h at 4°C) to remove the GAG chains from the core proteins by β-elimination. After neutralization with glacial acetic acid, concentrated ammonium bicarbonate was added and after the bubbling stopped, samples were analyzed on a Sepharose CL-6B column (1 cm × 120 cm) equilibrated in 0.5 M NH_4HCO_3 to compare the relative size of the protein standards.

ENZYMATIC DEPOLYMERIZATION OF HS CHAINS

The purified HS samples (100 μg) were dissolved in 100 mM sodium acetate/0.2 M calcium acetate, pH 7.0 and incubated with 10 mU/ml of heparinase or hepritinase I in the same buffer at 37°C for 16 h and then a second aliquot of enzyme added and incubated for a further 4 h. The heparinase or heparitinase I digested HS sample was then passed over a BioGel P-6 column (1 cm × 120 cm) equilibrated with 0.25 M NH_4HCO_3 to compare the relative sizes of the heparin oligosaccharides.

DISACCHARIDE ANALYSIS USING STRONG ANION EXCHANGE CHROMATOGRAPHY (SAX-HPLC)

Samples (100 μg) were dissolved in 100 mM sodium acetate/0.2 M calcium acetate, pH 7.0. Heparinase, heparitinase I and II were all used at a concentration of 10 mU/ml in the same buffer. Each sample was sequentially digested for a recovery of disaccharides for SAX-HPLC analysis; for this the samples were digested at 37°C as follows: heparinase for 2 h, heparitinase I for 1 h, heparitinase II for 18 h, and finally an aliquot of each lyases for 6 h. Samples were run on a BioGel P-2 column (1 cm × 120 cm) equilibrated with 0.25 M NH_4HCO_3. The disaccharide peak was lyophilized and then dissolved in acidified water (pH 3.5 with HCl). This was passed over a ProPac PA-1 SAX-HPLC column (Dionex, USA), attached to a high pressure liquid chromatography system and the HS disaccharides eluted with a linear gradient 0–1.0 M NaCl, pH 3.5, over 60 min at a flow-rate of 1 ml/min. The peaks identified using HS disaccharides standards (Seikagaku, Tokyo, Japan) monitored at $A_{232\,nm}$.

REVERSE TRANSCRIPTION-PCR

Expression of endogenous HS chain biosynthesis enzymes were determined by RT-PCR of human osteoblast cell RNA. RNA was reverse transcribed to cDNA using the SuperScript III™ First-Strand Synthesis System (Invitrogen). cDNA samples were denatured at 95°C and amplified for 40 cycles with each cycle consisting of 30 s of denaturation at 94°C, 30 s of annealing at 55°C and 2 min of extension at 72°C using AmpliTaqGold DNA polymerase™ (ABI). The PCR primers for heparan sulfate 2-*O*-sulfotransferase 1 (HS2OST1) were TCCCGCTCGAAGCTAGAAAG and CGAGGGC-CATCCA-TTGTATG; heparan sulfate 6-*O*-sulfotransferase 1 (HS6ST 1) AGCGGACGT-TCAACCTCAAGT and GCGTAGTCGTACAGCTG-CATGT; heparan sulfate 6-*O*-sulfotransferase 2 (HS6ST2) TCTGGA-AAGTGCCAAGTCAAATC and ATGGCGAAATAAAGTTC-ATGTTG-AA; heparan sulfate 6-*O*-sulfotransferase 3 (HS6ST 3) ACAT-CACGCGGGCTTCTAACGT and GGCGGTCCCTCTGG-TGCTCTA; *N*-deacetylase/*N*-sulfotransferase 1 (NDST-1) TGGTCTTGGAT-GG-CAAACTG and CGCCAAGGTTTT-GTGGTAGTC; *N*-deacetylase/*N*-sulfotransferase 2 (NDST-2) CCTATTTGAAAAAA-GTGCCACCTACT and GCAGGGTTGGTGAGCACTGT; *N*-deacetylase/*N*-sulfotransferase 3 (NDST-3) ACCCTTCAGACCGAGCATACTC and CCCGGGACC-AAACATCTCTT; *N*-deacetylase/*N*-sulfotransferase 4 (NDST-4) AT-AAAGCCAATGAGAACAGCTT-ACC and GGTAATATGCAGCAAA-GGAG-ATTGA.

SURFACE PLASMON RESONANCE (SPR) ANALYSIS OF PROTEIN–SUGAR INTERACTIONS

Real time biomolecular interaction analyses were performed with an Autolab ESPR (Eco Chemie, The Netherlands) [Wink et al., 1998] equipped with a two-channel cuvette, with the sensor disk forming the base of the cuvette. In a kinetic measurement model, molecular interactions were monitored as SPR angle shifts (Δθ in mDeg) over time. The measured Δθ was proportionally related to the amount of adsorbed material with a mass sensitivity of 100 ng/cm^2 per 120 mDeg for protein and sugars. The measurements were conducted at room temperature and the noise level was 0.2 mDeg.

The sensor chips were gold-coated glass substrates purchased from Eco Chemie. The gold disks were cleaned in UV ozone for 5 min and then with piranha solution (3:1 solution of H_2O and H_2SO_4). A 1 mM binary biotin-containing thiol mixture of 10% biotin PEG disulfide (LCC Engineering & Trading GmbH, Switzerland) and 90% ethylene-glycol thiol (Sigma) in ethanol was deposited on the clean gold disk and incubation occurred overnight in an ethanol environment. The chips were then rinsed in ethanol and dried in N_2. Streptavidin (50 μl of 0.1 mg/ml) in PBS buffer was then allowed to react with the biotin-containing surface for 20 min to create a streptavidin monolayer. This layer was then used to immobilize biotinylated HS, followed by the injection of designated growth factors (50 μl, 200 nM) for 20 min. Rinsing steps with respective buffer were added before each reagents were change to remove the non-specific binding.

Heparan sulfate (10 mg) was dissolved in 1 ml 0.1 M MES, pH 5.5 and 300 μl 0.1 MES, pH 5.5, containing 2 mg/ml biotin-LC-hydrazide (Pierce), EDC (7 mg) was added to the mixture and incubated at room temperature for 2 h before addition of another 7 mg of EDC. After a further 2 h incubation, unincorporated biotin was removed with a desalting column (Amersham Pharmacia), followed by anion-exchange chromatography with a 5 ml Econo-Q cartridge (Bio-Rad). The column was washed with PBS containing 250 mM NaCl. The biotinylated HS fraction was eluted with PBS containing 2 M NaCl. The biotinylated HS fractions eluted from the anion-exchange column were applied to a desalting column, eluted with water and lyophilized.

RESULTS

PURIFICATION OF HS CHAINS

Proteoglycans (PGAGs) extracted from the three compartments of the human primary osteoblast cells were subjected to

anion-exchange chromatography. Material bound to the anion exchange column was eluted using a linear gradient of NaCl (Fig. 1A–C). A sharp symmetrical peak of 232 nm absorbance emerged from the anion-exchange matrix, peak fractions were pooled, concentrated and desalted with low salt buffer, and the carbazole test for uronic acids used to confirm the presence of different polysaccharides. These samples were then treated with neuraminidase, chondroitin ABC lyase and pronase and then again subjected to anion-exchange chromatography. HS glycosaminoglycans (HS GAGs) bound to the anion-exchange column were eluted using a linear gradient of NaCl (Fig. 1D–F) and the peak fractions pooled, concentrated and desalted with water, then quantified as above. The purified HS GAGs were treated with $NaBH_4$ and subsequent separation on Sepharose CL-6B demonstrated that the HS chains from medium, cell surface and matrix all eluted in a single peak with a K_{av} of 0.4, with little detectable difference in average length (corresponding to sizes approximately 35–38 kDa (data not shown)).

HEPARINASE TREATMENT OF HS SAMPLES

The enzyme heparinase cleaves HS where GlcNS (±6S)-IdoUA (2S) residues occur, although the enzyme is also active against GlcUA (2S), a rare constituent of HS. HS samples from the three compartments were incubated with heparinase and the products analyzed on a BioGel P-6 column. Figure 2A–C illustrates the profile of heparinase resistant fragments derived from media, cell surface and matrix HS. This enzyme generated a similar pattern of resistant fragments ranging in size from disaccharide (dp2) to approximately hexasaccharide (dp6) in a very similar pattern in soluble, cell surface, and matrix HS, albeit the amount of di-, tetra-, and hexasaccharide in matrix HS was different from the soluble and cell surface HS (Table I).

HEPARITINASE I TREATMENT OF HS SAMPLES

Heparitinase I mostly cleaves HS at hexosaminidic to glucuronic acid residue linkages. HS samples from the three compartments were incubated with heparitinase I and the products analyzed on a BioGel

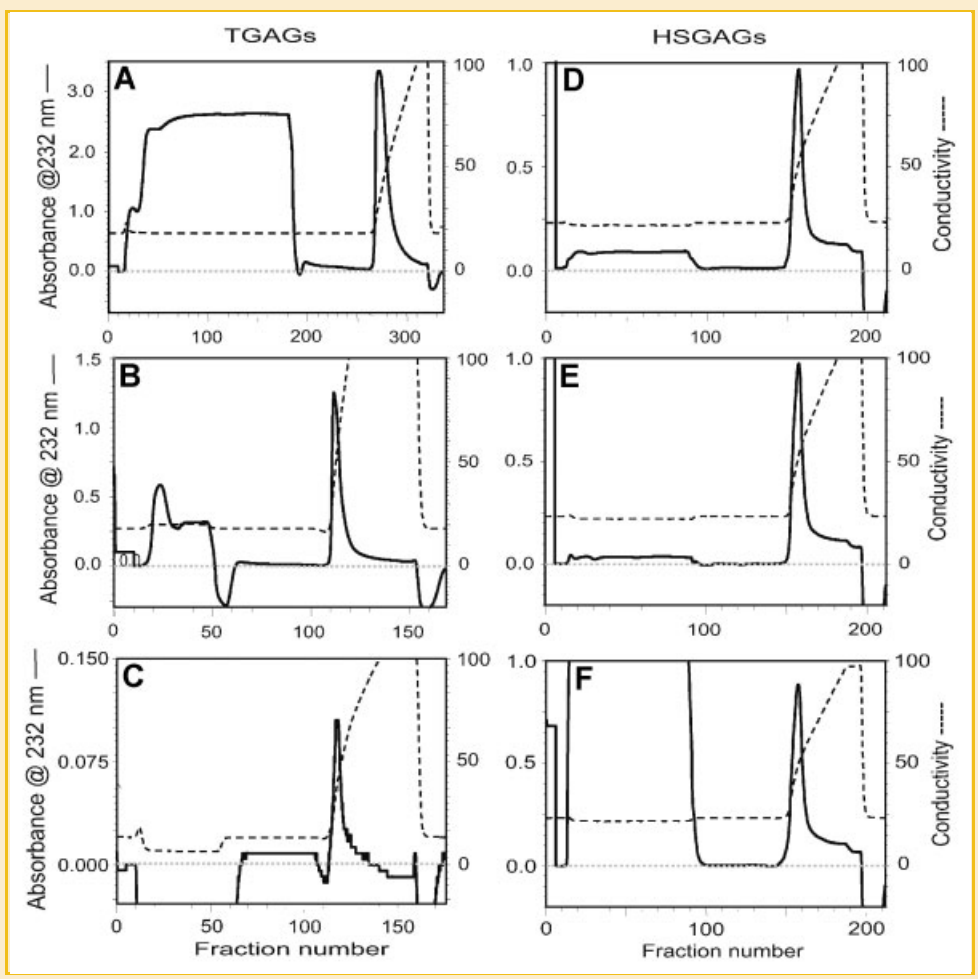

Fig. 1. Isolation of proteoglycans, total glycosaminoglycans (TGAGs; A–C) and HS glycosaminoglycans (HSGAGs; D–F) by anion-exchange chromatography. Extracts from the three compartments were applied to the column and washed with Tris–HCl buffer containing a low (150 mM) NaCl concentration. After washing with low salt buffer, the bound TGAGs and HSGAGs were eluted with a linear gradient of NaCl from 150 mM to 1 M. Peaks representing retained fractions (monitored at 232 nm and tested for uronic acid confirmed the presence of glycosaminoglycans) were collected and subjected to further purification.

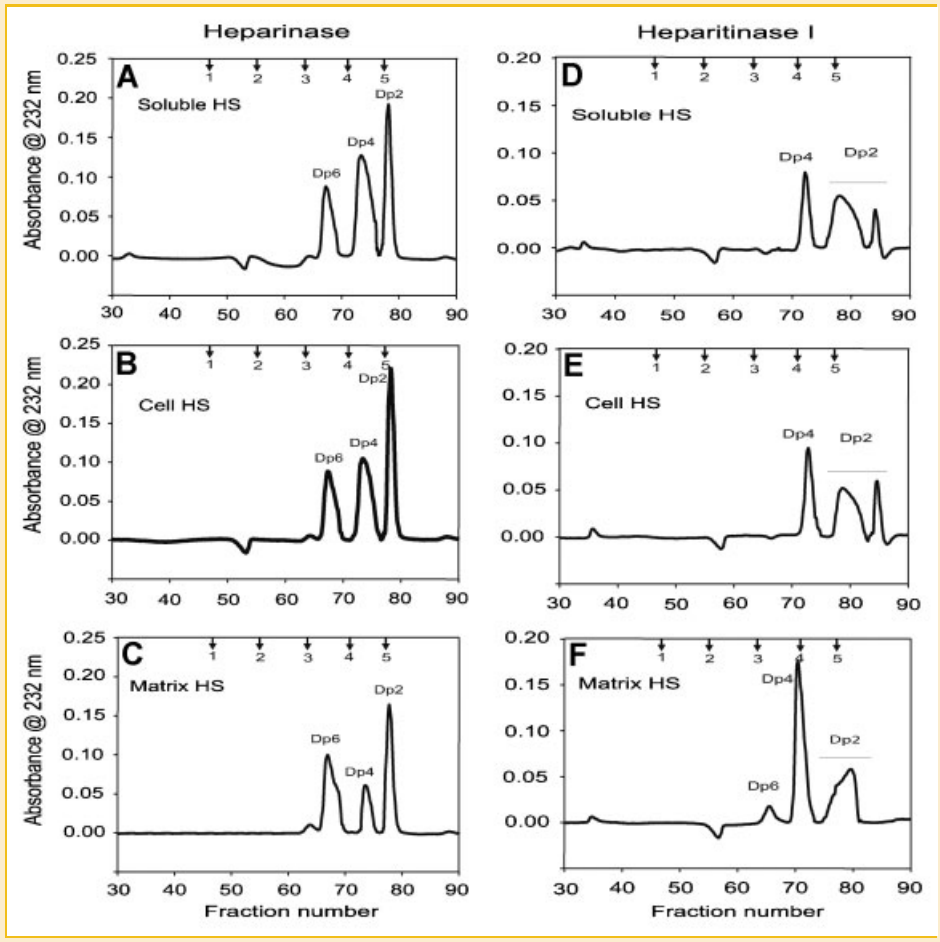

Fig. 2. Bio-Gel P6 gel filtration chromatography of oligosaccharides produced by heparinase digestion [soluble (A), cell surface (B), and matrix (C) HS] and heparitinase I [soluble (D), cell surface (E), and matrix (F) HS]. Heparinase cleaves HS essentially at GlcNS(±6S)-IdoUA(2S) residues. This enzyme generated resistant fragments ranging in size from disaccharide (dp2) to approximately hexasaccharide (dp6). Heparitinase I mostly cleaves HS at Glc(NS or NAc, ±6S)-GlcUA residues. This enzyme generated resistant fragments ranging in size from disaccharides (dp2) to hexasaccharides (dp6). The absorbance area under each peak was compared with the heparin oligosaccharide standards absorbance area to calculate the percentage composition of each oligosaccharide. The arrow indicates the elution position of heparin oligosaccharide standards (1. dp10; 2. dp8; 3. dp6; 4.dp4 and 5. dp2). dp, degree of polymerization.

P-6; Figure 2D–F illustrates the profile of heparitinase I-resistant fragments derived from media, cell surface and ECM. Approximately 50% of the HS chains from the soluble and cell surface preparations were digested to disaccharides (Fig. 2D,E). The splitting of the disaccharide peak is due to almost complete resolution of the disaccharides into mono- and tri-sulfated disaccharide. The elution profile of the soluble and cell surface HS displayed similar patterns of resistant fragments, ranging in size from dp2 to dp4 in very similar proportions. However, the matrix HS yielded fragments ranging in size from dp2 to dp6 in a distinct proportion (Fig. 2F; Table II).

TABLE I. Percentage Composition of Oligosaccharide Produced by Heparinase Digestion of Soluble, Cell Surface, and Matrix HS*

Heparinase-digested HO3–HS samples	Dp2 (%)	Dp4 (%)	Dp6 (%)
Soluble HS	15	35	50
Cell HS	18	30	52
Matrix HS	14	14	72

*The area under each peak was compared with the heparin oligosaccharide standards to calculate the percentage composition of each oligosaccharides.

SAX-HPLC ANALYSIS OF DISACCHARIDES

To investigate potential differences in the disaccharide content of the HS chains between the three compartments of the same cell

TABLE II. Percentage Composition of Oligosaccharides Produced by Heparitinase I Digestion of Soluble, Cell Surface, and Matrix HS*

Heparitinase I-digested HO3–HS samples	Dp2 (%)	Dp4 (%)	Dp6 (%)
Soluble HS	49	51	n.d.
Cell HS	46	54	n.d.
Matrix HS	18	66	16

n.d., not detected.
*The area under each peak was compared with the heparin oligosaccharide standards to calculate the percentage composition of each oligosaccharides.

culture, HS chains were exhaustively digested with a mixture of heparinase, heparitinase I and II. The disaccharides were separated on a BioGel P-2, and the separated disaccharides were again separated with strong anion-exchange chromatography, with the resulting peaks identified by reference to standards. Nonsulfated HexUA-GlcNAc was the most common disaccharide from the three sources of HS chains, with distinct differences in HS chain composition derived from the medium, cell surface and ECM (Fig. 3B–D; Table III).

EXPRESSION OF HS BIOSYNTHETIC ENZYMES

The amounts and positioning of HS sulfate groups within chains are determined during biosynthesis. This occurs in the Golgi compartment, and can be divided into chain initiation, polymerization and modification [Lindahl et al., 1998]. In HO3 cells, of the first modification enzymes, NDST-1, NDST-2 isoforms were highly expressed; NDST-3 to a lesser extent, and NDST-4 was not detectable. Furthermore, the C-5 epimerase is expressed at low levels, but HS2OST more strongly. The final modification enzyme, HS6ST has four isoforms, but only HS6ST-1 was expressed in HO3 cells (Fig. 4).

ANALYSIS OF HS BINDING AFFINITY FOR GROWTH FACTORS

The possibility that the small structural differences identified between the three different preparations of HS from same cell culture reflected differences in their growth factor binding capabilities was investigated using an in vitro ligand-binding assay. The three HS preparations (soluble, cell, and ECM) were tested for their capacity to bind the three growths factors, FGF1, FGF2, and BMP2, all known to be expressed by osteoblasts. Real time binding analysis was carried out using SPR, wherein biotin thiol-coated gold sensor chips were used as a platform for immobilized streptavidin [Su et al., 2005]. Using a biotin–streptavidin–biotin bridge, biotinylated HS could be immobilized on the sensor chip. The growth factors (200 nM) were then added onto the immobilized HS and incubated for 20 min. Real time binding was monitored by measuring the change in the minimum reflectance angle (θ) over time. Figure 5 depicts representative binding curves of the growth

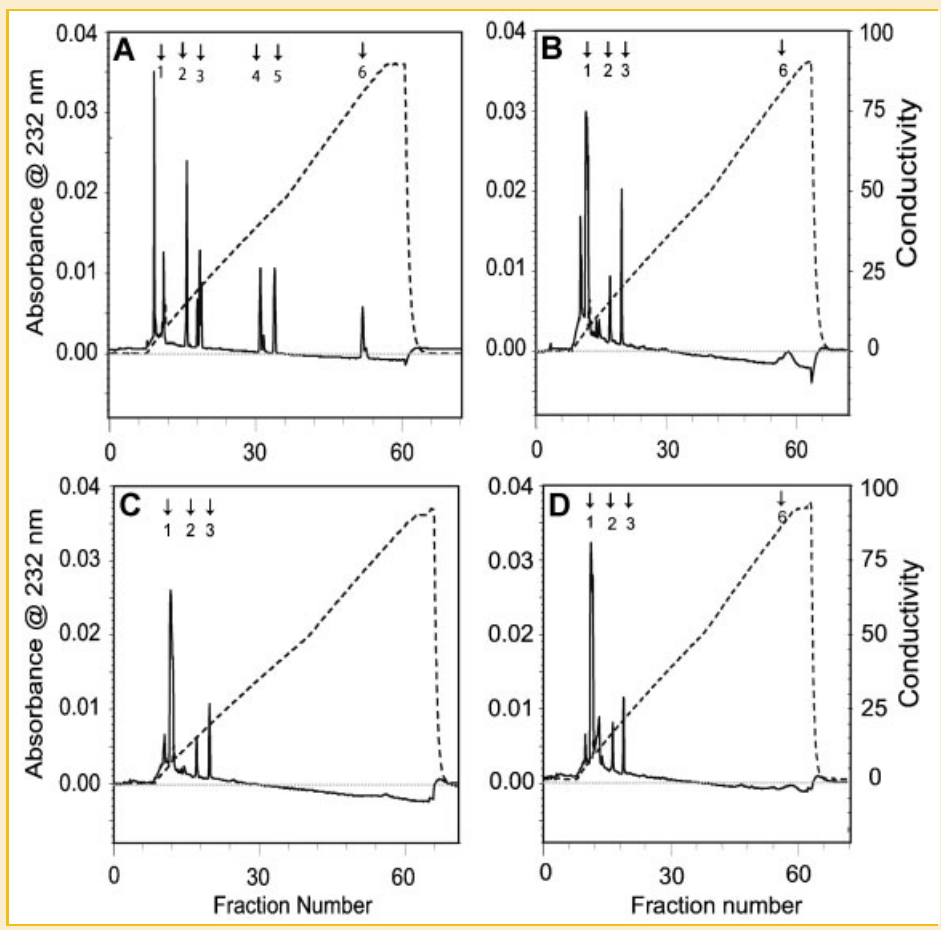

Fig. 3. HS was completely depolymerized with a mixture of heparan lyases. The disaccharides were isolated on Bio-Gel P2 columns and fractionated by SAX-HPLC. Disaccharides were identified by comparison of their elution position relative to those of known disaccharide standards. A: Unsaturated HS disaccharides standards; (1) HexA-GlcNAC, (2) HexA-GlcNS, (3) HexA-GlcNAc(6S), (4) HexA-GlcNS(6S), (5) HexA(2S)-GlcNS, (6) HexA(2S)-GlcNS(6S). Heparin lyase-treated (B) soluble, (C) cell surface and (D) matrix HS disaccharides. The area under each peak was integrated to calculate the percentage of each disaccharide. Arrows indicated the elution positions of standard disaccharides. ⊕ Unidentified peaks.

TABLE III. Lyase-Derived Disaccharide Percentage Compositions of Soluble, Cell Surface, and Matrix HS*

No.	Disaccharide standards	% Composition		
		Soluble HS	Cell HS	Matrix HS
1	ΔHexUA-GlcNAc	45	54	50
2	ΔHexUA-GlcNSO3	15	14	13
3	ΔHexUA-GlcNAc(6S)	30	24	17
4	ΔHexUA-GlcNSO3(6S)	n.d.	n.d.	n.d.
5	ΔHexUA(2S)-GlcNSO3	n.d.	n.d.	n.d.
6	ΔHexUA(2S)-GlcNSO3(6S)	10	3	5
7	Unknown	10	5	15

n.d., not detected.
*The area under each peak was integrated to calculate the percentage of each disaccharides.

factors with the various HSs. The rise of the curves over time shows the association of the growth factors to the immobilized HS. Rinsing the surface at the end of each 20 min incubation removed unstable binding, causing the angle shift to drop, with the difference in the angle shift before binding and after rinsing recorded. Control experiments were conducted to examine the non-specific binding of the growth factors on the streptavidin surface alone; notably there was no significant angle shift observed, suggesting no non-specific binding to the streptavidin layer.

As shown by the curves in Figure 5, FGF1 does not bind strongly to any of the HSs (Fig. 5A), as evidenced by the small angle shift. FGF2 (Fig. 5B) and BMP2 (Fig. 5C), in contrast however, bind to the three HSs more strongly. Binding signals generated by FGF2 on soluble HS, cell HS, and ECM HS were 116.25 ± 12.1, 64.5 ± 9.3, and 70.67 ± 11.6 mDeg, respectively ($n = 4–6$; Fig. 5D). Similar binding of BMP2 to the three types of HS was also observed, with binding signals of 125.5 ± 18.55, 120.3 ± 6.35, and 110.6 ± 24 mDeg recorded, respectively ($n = 4–5$; Fig. 5D). In addition to the distinct binding levels of the different growth factors, we also observed different binding kinetics between the BMP2 and FGF2. BMP2 took longer to approach equilibrium compared with FGF2, which may be due to a slower binding kinetic, or greater diffusion limitation of the BMP2 to the sensor surface due to its larger molecular size and surface charge.

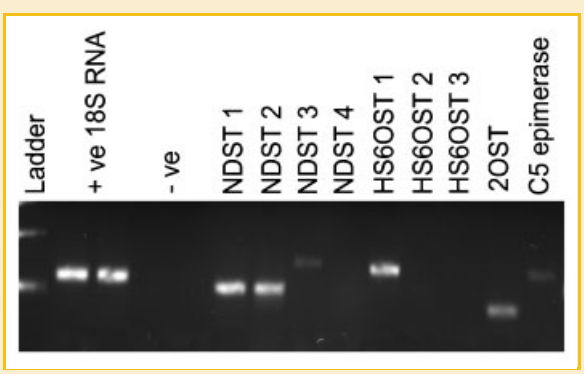

Fig. 4. Endogenous expression of HS chain biosynthesis enzymes in human primary osteoblast cell cultures.

DISCUSSION

HS biosynthesis is a complex multi-step process that occurs in a very specific and sequential manner via membrane-bound enzymes in the endoplasmic reticulum and Golgi apparatus. In this study we describe an analysis of the structural and ligand-binding properties of HS chains purified from three compartments of cultured adult primary human osteoblasts, namely the soluble, cell surface, and matrix fractions. We show that they are structurally similar at the gross level, yet different at the finer dissacharide level. These differences may also be functionally significant due to the altered ligand-binding activity we observed.

Heparinase cleaves HS chains with sulfate-rich regions at *N*-sulfated-glucosamine/sulfated-iduronic acid linked regions. The size of the fragments generated, compared to the undigested chain, indicates the frequency of these areas of high sulfation. Separation of the HS chains from soluble, cell surface, and matrix after digestion with heparinase gave nearly identical profiles. However, the proportions of di-, tetra-, and hexasaccharide fractions formed by heparinase cleavage were different in the soluble, cell surface, and matrix HS preparations. The fragments from HO3 soluble, cell surface, and matrix HS were similar in size, but the distribution of these domains within the molecules were different. All three HSs showed less sensitivity to heparinase, with ~15% of the linkages reduced to disaccharides and 50–70% to hexasaccharides. This may indicate a lack of closely aligned heparinase-susceptible sites in the soluble, cell surface, and matrix HS as they probably exists in only relatively small clusters. This is similar to previous reports on skin HS, in which the IdoUA residue (that is essential for heparinase cleavage) is present in low concentrations (6.5–10% of total HexUA) [Turnbull and Gallagher, 1990, 1991].

In contrast to heparinase, heparitinase I cleaves HS chains in *N*-acetylated regions of low sulfation. It therefore leaves areas of high sulfation intact, allowing their size to be estimated. Separation of the HS chains from the soluble and cell surface fractions after digestion with heparitinase I gave nearly identical profiles, with the matrix HS differing more markedly. Heparitinase I cleaved 50% material from soluble and cell surface into disaccharides units. This is similar to the 63% disaccharide content obtained with skin fibroblasts [Turnbull and Gallagher, 1990] but substantially less than the 78% obtained for endothelial HS [Lindblom and Fransson, 1990]. However, matrix HS was degraded to 18% disaccharides, leaving large proportions of tetra- (66%), and octasaccharide (16%) units with their resistant domains of high sulfation. The susceptible sites were highly contiguous, and the resistant fragments alternated to form tetrasaccharides. This is consistent with the finding of relatively few or high areas of heparinase susceptibility, and suggests that the sulfated regions are of similar size in both the soluble and cell surface fractions. These results suggest that the HS chains derived from the soluble and cell surface compartments contain domains of *N*-sulfation that are separated by longer sequences of low sulfation compared to those derived from the matrix compartment.

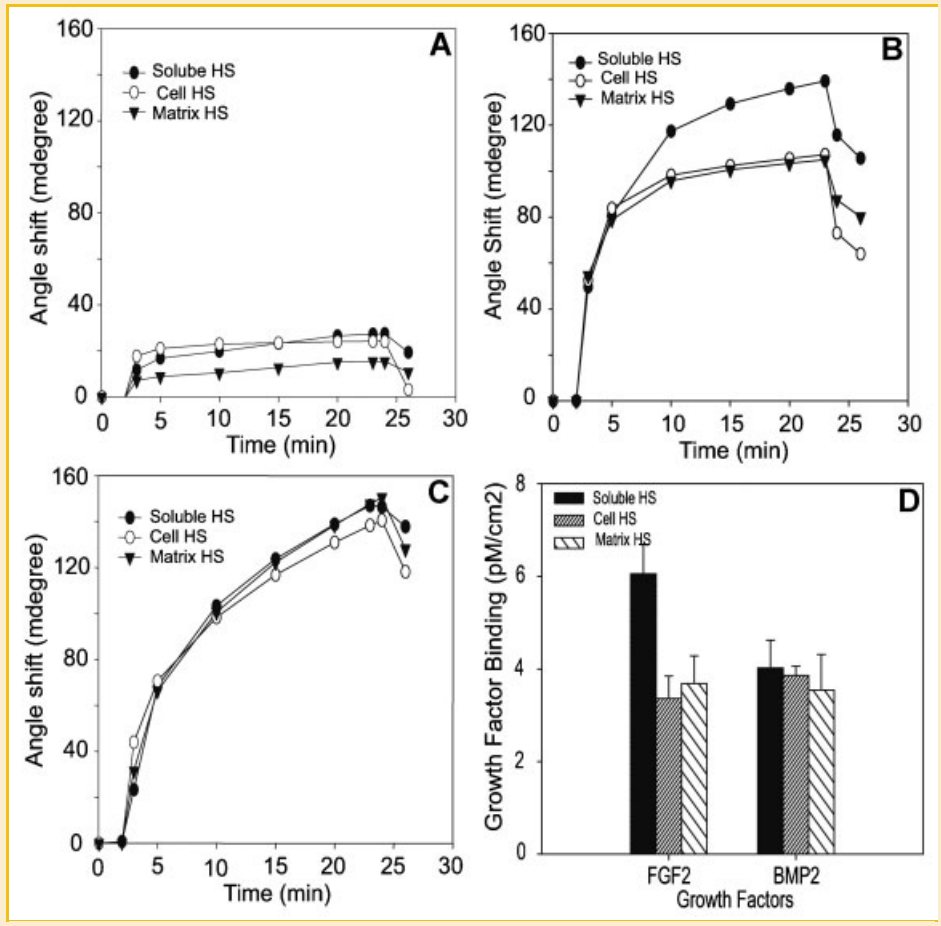

Fig. 5. Binding curves of FGF1, FGF2, and BMP2 (200 nM) to various HS variants purified from the soluble, cell surface and matrix components of human proary osteoblast cultures. A: Binding of FGF1 to various HS shows minimum binding. B,C: Binding of FGF2 and BMP2 shows relatively strong interactions to various HS with different binding kinetic between FGF2 and BMP2. D: Binding capacity of FGF2 and BMP2 to various HSs was calculated by converting the measured angles shift to molecular mass change using the SPR mass sensitivity factor (120 mDeg corresponding to 100 ng/cm^2 mass increase) and the growth factor molecular weight.

Disaccharide sequence analysis of soluble, cell surface, and matrix HS following digestion were performed and the identities of each disaccharide confirmed by co-injection with individual disaccharide standards. The unmodified sequence of ΔHexUA-GlcNAc (NAc domains) is predominant for all the three species of HS. This unmodified sequence is a structural element common to many HSs [Rabenstein, 2002]. In skin fibroblast HS, this sequence is from 8 to 11 disaccharides in length [Turnbull and Gallagher, 1990]; in endothelial HS, it is 10–11 disaccharides in length [Lindblom and Fransson, 1990], and in rat liver HS it is 8–11 disaccharide in length [Lyon et al., 1994]. Here, the percentage compositions of ΔHexUA-GlcNAc, ΔHexUA-GlcNS, ΔHexUA2S-GlcNAc, and ΔHexUA2S-GlcNS6S within soluble HS was very different from those of cell surface and matrix HS. Five to 15% unknown disaccharides were identified in all three species of HS; these disaccharides may be the *N*-unsubstituted glucosamine residues. The *N*-unsubstituted glucosamine ($GlcNH_3^+$) unit has been previously reported in native HS [Toida et al., 1997; Westling and Lindahl, 2002] and may play an important biological and pathological role. Fortunately, the substrate specificities of heparinases against *N*-unsubstituted glucosamine residues in HS have been identified [Wei et al., 2005] which may help yield important structural information in the future.

Taken together, our data suggest the possibility of yet another model for the structure of HS. The generic model that posited regions of high sulfation interspersed with acetylated regions [Turnbull and Gallagher, 1991] was recently modified to include transition zones between the areas of low and high sulfation [Murphy et al., 2004]. Other models have included that for liver HS [Lyon et al., 1994], where the distal end of the sugar is much more sulfated than the proximal end and creates an asymmetric chain, and models where adjacent sulfated regions cooperate to bind either a single ligand, or a dimer, as for interferon-χ, platelet factor 4 and interleukin-8 [Lindahl et al., 1998]. Our digestion results suggest that there may exists yet another form of HS from mature, adult tissues whose structure more resembles long stretches of transition zone, with domains on average shorter than those of "standard" S-domains, which are usually 8–12 disaccharide units [Powell et al., 2004].

Knowledge of the variations in composition and organization of HS from different cells and tissues is becoming increasingly important as attempts are made to elucidate the relationship between HS structure and function. Each tissue type bears a unique

complement of HS structures that may also vary at different stages of tissue development [Brickman et al., 1998a; Lindahl et al., 1998]; thus for example, differing complements of HS appear to change the way that heparin/HS-dependent growth factors such as the FGFs exert their mitogenic and differentiative effects within developing tissues [Nurcombe et al., 1993]. Structural analyses of HS chains have been limited mainly to general size and composition, due to lack of analytical methodologies with sufficient sensitivity to sequence the small quantities of HS that can be recovered from HSPGs on cell surfaces and in the ECM.

HSPGs participate in several cellular events, including organogenesis [Perrimon and Bernfield, 2000], angiogenesis [Robinson and Stringer, 2001], growth factor/cytokine action, cell adhesion [Couchman, 2003], lipid metabolism and wound healing [Rosenberg et al., 1997]. All these activities are manifested via specific interactions of HS chains at the cell surface with ECM effector molecules [Bernfield et al., 1999], particularly the vast array of growth factors that require subsequent transfer to high-affinity signaling receptors [Zako et al., 2003]. The interactions between mitogens and HS have been studied extensively for the fibroblast growth factors (FGF) family, for the FGFs-1, -2, -4, -7, -8, -10, and -18 have all been shown to bind to HS [Powell et al., 2002].

FGFs and FGFRs also play critical roles in the control of many fundamental osteogenic processes, including osteoblast proliferation, differentiation and migration [Cool and Nurcombe, 2005; Jackson et al., 2006a]. HS purified from differentiating MC3T3-E1 pre-osteoblast cells enhances differentiation in non-confluent pre-osteoblast cells [Jackson et al., 2007], and also increases trabecular bone volume by 20% from a single application into mid-diaphyseal femoral fractures [Jackson et al., 2006b]. Mitogens crucial to tissue regeneration such as the platelet-derived growth factors (PDGFs), as well as bone morphogenetic protein-7 (BMP-7) have also been shown to interact with HS [Feyzi et al., 1997; Irie et al., 2003].

As the HS chain grows during its synthesis, it is modified by series of enzymes; the first modification reaction is catalyzed by NDST, which removes acetyl groups from *N*-acetylglucosamine residues, which are then sulfated through the *N*-sulfotransferase activity. Among the four isoforms of NDST (NDSTs-1–4), only NDST-1, NDST-2 were expressed significantly in the HO3 cells, with NDST-3 expressed to a lesser extent. NDST-1 and NDST-2 mRNA are expressed in all embryonic and adult tissues that have been examined, albeit at different levels [Aikawa et al., 2001; Kusche-Gullberg et al., 1998]. NDSTs-3 and -4 appear to be more restricted [Grobe et al., 2002]. The second modification reaction is catalyzed by C-5 epimerase, which modifies the C-5 epimerization of glucuronic acid into iduronic acid. The expression of C-5 epimerase is relatively slight in HO3 cells. The third modification reaction is catalyzed by HS2OST, which modifies the 2-*O*-sulfation of glucuronic acid/iduronic acid, but preferentially iduronic acid. In HO3 cells, HS2OST is expressed significantly even though the HPLC showed the lower presence of 2-*O*-sulfated disaccharide. This might be due a lack of glucuronic acid to iduronic acid conversion, because of the low expression of C-5 epimerase in HO3 cells. The final modification reaction is catalyzed by HS6STs-1-3, which add sulfates onto glucosamine groups. HS6ST-1 transfers sulfates preferentially to position 6 of GlcNS and GlcNAc residues, HS6ST-2 transfers preferentially to position 6 of GlcNS residues and HS6ST-3 activity appears to be intermediate between those of HS6ST-1 and HS6ST-2 [Habuchi et al., 2000; Zhang et al., 2001]. This is consistent with the results obtained here, where HO3 cells only express HS6ST-1, and the disaccharide analysis confirmed the presence of 6-sulfate in 15–30% ΔHexUA-GlcNAc(6S) and 3–10% ΔHexUA(2S)-GlcNS(6S).

Generally the ratio of iduronic acid to glucuronic acid is low in HS, and the numbers of *N*-sulfated glucosamines are approximately equal. The current generic model for HS chains posits IdoA- and $GlcNSO_3$-containing regions that are highly sulfated (S-domains), alternating with regions that are predominantly acetylated with relatively low sulfates, like pearls along a necklace [Gallagher, 2006]. There is also a minor proportion of mixed sequences, in transition regions between the high and low sulfate regions which contain both $GlcNSO_3$ and GlcNAc [Murphy et al., 2004]. The S-domains may contain heparin-like trisulfated disaccharides as well as disulfated saccharides. Ido2S-$GlcNSO_3$ and C-6 sulfation of GlcN NSO_3 may also occur in the mixed regions. The deacetylation of GlcNAc to yield an unsubstituted amine occurs in the mixed regions and the *N*-acetylated domains [Westling and Lindahl, 2002]. The structural similarities and differences observed between the HS isolated from the different osteoblast compartments suggest that HS chains present in the culture medium and matrix are not only derived from the proteolytic cleavage of the cell surface HSPG, or from subsequent extracellular endosulfatase modification [Ai et al., 2003; Uchimura et al., 2006], but are directly secreted from the cell into the medium. Furthermore, the amount of HS, as well as its composition in these pools changes when growing cells reach confluence. A similar result was reported by Brickman et al. [1998b] who isolated two separate pools of HS from immortalized neuroepithelial cells derived from embryonic day 10 mice, one from cells in log-phase growth, which greatly potentiated the activity of FGF2, and a second from contact-inhibited cells, which preferentially activated FGF1.

The specific interaction between HS and various growth factors/cytokines have attracted much attention. The nature of many protein-HS interactions has been characterized, including those that require a specific and defined HS sulfation pattern for binding, such as the fibroblast growth factor (FGF) family [Ornitz et al., 1992; Guimond et al., 1993]. FGF2 is known interact with *N*-sulfoglucosamine (GlcNS) and 2-*O*-sulfated iduronate residues (IdoUA(2S) in heparin and HS [Turnbull et al., 1992]. Here we show that cell surface and matrix HS bind significantly to FGF-2 and BMP-2 but not FGF-1. FGF-2 however bound soluble HS with a 1.7-fold higher affinity than either cell surface or matrix HS. This higher binding may be because soluble HS contains more *N*-sulfoglucosamine and 2-*O*-sulfated iduronate residues than cell surface and matrix HS.

In conclusion, we show that HS chains purified from three compartments of human primary osteoblast cultures are similar in terms of their fine structure yet contain differences in the structure of the HS chain domains that may reflect differences in their ligand binding.

ACKNOWLEDGMENTS

This work was supported by the Biomedical Research Council, A*STAR (Agency for Science Technology and Research), Singapore, and the Institute of Medical Biology, A*STAR, Singapore. The authors also wish to thank members of the VNSC lab for their continued support.

REFERENCES

Ai X, Do AT, Lozynska O, Kusche-Gullberg M, Lindahl U, Emerson CP, Jr. 2003. QSulf1 remodels the 6-O sulfation states of cell surface heparan sulfate proteoglycans to promote Wnt signaling. J Cell Biol 162:341–351.

Aikawa J, Grobe K, Tsujimoto M, Esko JD. 2001. Multiple isozymes of heparan sulfate/heparin GlcNAc N-deacetylase/GlcN N-sulfotransferase. Structure and activity of the fourth member, NDST4. J Biol Chem 276: 5876–5882.

Ashikari-Hada S, Habuchi H, Kariya Y, Itoh N, Reddi AH, Kimata K. 2004. Characterization of growth factor-binding structures in heparin/heparan sulfate using an octasaccharide library. J Biol Chem 279:12346–12354.

Bernfield M, Gotte M, Park PW, Reizes O, Fitzgerald ML, Lincecum J, Zako M. 1999. Functions of cell surface heparan sulfate proteoglycans. Annu Rev Biochem 68:729–777.

Berry D, Shriver Z, Venkataraman G, Sasisekharan R. 2004. Quantitative assessment of FGF regulation by cell surface heparan sulfates. Biochem Biophys Res Commun 314:994–1000.

Brickman YG, Ford MD, Gallagher JT, Nurcombe V, Bartlett PF, Turnbull JE. 1998a. Structural modification of fibroblast growth factor-binding heparan sulfate at a determinative stage of neural development. J Biol Chem 273: 4350–4359.

Brickman YG, Nurcombe V, Ford MD, Gallagher JT, Bartlett PF, Turnbull JE. 1998b. Structural comparison of fibroblast growth factor-specific heparan sulfates derived from a growing or differentiating neuroepithelial cell line. Glycobiology 8:463–471.

Casu B, Lindahl U. 2001. Structure and biological interactions of heparin and heparan sulfate. Adv Carbohydr Chem Biochem 57:159–206.

Cool SM, Nurcombe V. 2005. The osteoblast-heparan sulfate axis: Control of the bone cell lineage. Int J Biochem Cell Biol 37:1739–1745.

Couchman JR. 2003. Syndecans: Proteoglycan regulators of cell-surface microdomains? Nat Rev Mol Cell Biol 4:926–937.

Esko JD, Lindahl U. 2001. Molecular diversity of heparan sulfate. J Clin Invest 108:169–173.

Esko JD, Selleck SB. 2002. Order out of chaos: Assembly of ligand binding sites in heparan sulfate. Annu Rev Biochem 71:435–471.

Feyzi E, Lustig F, Fager G, Spillmann D, Lindahl U, Salmivirta M. 1997. Characterization of heparin and heparan sulfate domains binding to the long splice variant of platelet-derived growth factor A chain. J Biol Chem 272: 5518–5524.

Gallagher JT. 2006. Multiprotein signalling complexes: Regional assembly on heparan sulphate. Biochem Soc Trans 34:438–441.

Grobe K, Ledin J, Ringvall M, Holmborn K, Forsberg E, Esko JD, Kjellen L. 2002. Heparan sulfate and development: Differential roles of the N-acetylglucosamine N-deacetylase/N-sulfotransferase isozymes. Biochim Biophys Acta 1573:209–215.

Guimond S, Maccarana M, Olwin BB, Lindahl U, Rapraeger AC. 1993. Activating and inhibitory heparin sequences for FGF-2 (basic FGF). Distinct requirements for FGF-1, FGF-2, and FGF-4. J Biol Chem 268:23906–23914.

Habuchi H, Tanaka M, Habuchi O, Yoshida K, Suzuki H, Ban K, Kimata K. 2000. The occurrence of three isoforms of heparan sulfate 6-O-sulfotransferase having different specificities for hexuronic acid adjacent to the targeted N-sulfoglucosamine. J Biol Chem 275:2859–2868.

Iozzo RV. 2001. Heparan sulfate proteoglycans: Intricate molecules with intriguing functions. J Clin Invest 108:165–167.

Irie A, Habuchi H, Kimata K, Sanai Y. 2003. Heparan sulfate is required for bone morphogenetic protein-7 signaling. Biochem Biophys Res Commun 308:858–865.

Jackson RA, Nurcombe V, Cool SM. 2006a. Coordinated fibroblast growth factor and heparan sulfate regulation of osteogenesis. Gene 379: 79–91.

Jackson RA, McDonald MM, Nurcombe V, Little DG, Cool SM. 2006b. The use of heparan sulfate to augment fracture repair in rat fracture model. J Orthop Res 24:636–644.

Jackson RA, Murali S, van Wijnen AJ, Stein GS, Nurcombe V, Cool SM. 2007. Heparan sulfate regulates the anabolic activity of MC3T3-E1 preosteoblast cells by induction of Runx2. J Cell Physiol 210:38–50.

Kusche-Gullberg M, Eriksson I, Pikas DS, Kjellen L. 1998. Identification and expression in mouse of two heparan sulfate glucosaminyl N-deacetylase/N-sulfotransferase genes. J Biol Chem 273:11902-11907.

Lindahl U, Kusche-Gullberg M, Kjellen L. 1998. Regulated diversity of heparan sulfate. J Biol Chem 273:24979–24982.

Lindblom A, Fransson LA. 1990. Endothelial heparan sulphate: Compositional analysis and comparison of chains from different proteoglycan populations. Glycoconj J 7:545–562.

Lyon M, Deakin JA, Gallagher JT. 1994. Liver heparan sulfate structure. A novel molecular design. J Biol Chem 269:11208–11215.

Lyon M, Rushton G, Askari JA, Humphries MJ, Gallagher JT. 2000. Elucidation of the structural features of heparan sulfate important for interaction with the Hep-2 domain of fibronectin. J Biol Chem 275:4599–4606.

Murphy KJ, Merry CL, Lyon M, Thompson JE, Roberts IS, Gallagher JT. 2004. A new model for the domain structure of heparan sulfate based on the novel specificity of K5 lyase. J Biol Chem 279:27239–27245.

Nurcombe V, Ford MD, Wildschut JA, Bartlett PF. 1993. Developmental regulation of neural response to FGF-1 and FGF-2 by heparan sulfate proteoglycan. Science 260:103–106.

Ornitz DM, Yayon A, Flanagan JG, Svahn CM, Levi E, Leder P. 1992. Heparin is required for cell-free binding of basic fibroblast growth factor to a soluble receptor and for mitogenesis in whole cells. Mol Cell Biol 12:240–247.

Ostrovsky O, Berman B, Gallagher J, Mulloy B, Fernig DG, Delehedde M, Ron D. 2002. Differential effects of heparin saccharides on the formation of specific fibroblast growth factor (FGF) and FGF receptor complexes. J Biol Chem 277:2444–2453.

Perrimon N, Bernfield M. 2000. Specificities of heparan sulphate proteoglycans in developmental processes. Nature 404:725–728.

Powell AK, Fernig DG, Turnbull JE. 2002. Fibroblast growth factor receptors 1 and 2 interact differently with heparin/heparan sulfate. Implications for dynamic assembly of a ternary signaling complex. J Biol Chem 277:28554–28563.

Powell AK, Yates EA, Fernig DG, Turnbull JE. 2004. Interactions of heparin/heparan sulfate with proteins: Appraisal of structural factors and experimental approaches. Glycobiology 14:17R–30R.

Pye DA, Gallagher JT. 1999. Monomer complexes of basic fibroblast growth factor and heparan sulfate oligosaccharides are the minimal functional unit for cell activation. J Biol Chem 274:13456–13461.

Rabenstein DL. 2002. Heparin and heparan sulfate: Structure and function. Nat Prod Rep 19:312–331.

Robinson CJ, Stringer SE. 2001. The splice variants of vascular endothelial growth factor (VEGF) and their receptors. J Cell Sci 114:853–865.

Rosenberg RD, Shworak NW, Liu J, Schwartz JJ, Zhang L. 1997. Heparan sulfate proteoglycans of the cardiovascular system. Specific structures emerge but how is synthesis regulated? J Clin Invest 100:S67–S75.

Su X, Wu YJ, Robelek R, Knoll W. 2005. Surface plasmon resonance spectroscopy and quartz crystal microbalance study of MutS binding with single thymine-guanine mismatched DNA. Front Biosci 10:268–274.

Toida T, Yoshida H, Toyoda H, Koshiishi I, Imanari T, Hileman RE, Fromm JR, Linhardt RJ. 1997. Structural differences and the presence of unsubstituted amino groups in heparan sulphates from different tissues and species. Biochem J 322(Pt 2):499–506.

Turnbull JE, Gallagher JT. 1990. Molecular organization of heparan sulphate from human skin fibroblasts. Biochem J 265:715–724.

Turnbull JE, Gallagher JT. 1991. Distribution of iduronate 2-sulphate residues in heparan sulphate. Evidence for an ordered polymeric structure. Biochem J 273(Pt 3):553–559.

Turnbull JE, Fernig DG, Ke Y, Wilkinson MC, Gallagher JT. 1992. Identification of the basic fibroblast growth factor binding sequence in fibroblast heparan sulfate. J Biol Chem 267:10337–10341.

Uchimura K, Morimoto-Tomita M, Bistrup A, Li J, Lyon M, Gallagher J, Werb Z, Rosen SD. 2006. HSulf-2, an extracellular endoglucosamine-6-sulfatase, selectively mobilizes heparin-bound growth factors and chemokines: Effects on VEGF, FGF-1, and SDF-1. BMC Biochem 7:2.

Walker A, Turnbull JE, Gallagher JT. 1994. Specific heparan sulfate saccharides mediate the activity of basic fibroblast growth factor. J Biol Chem 269:931–935.

Wei Z, Lyon M, Gallagher JT. 2005. Distinct substrate specificities of bacterial heparinases against N-unsubstituted glucosamine residues in heparan sulfate. J Biol Chem 280:15742–15748.

Westling C, Lindahl U. 2002. Location of N-unsubstituted glucosamine residues in heparan sulfate. J Biol Chem 277:49247–49255.

Whitelock JM, Iozzo RV. 2005. Heparan sulfate: A complex polymer charged with biological activity. Chem Rev 105:2745–2764.

Wink T, van Zuilen SJ, Bult A, van Bennekom WP. 1998. Liposome-mediated enhancement of the sensitivity in immunoassays of proteins and peptides in surface plasmon resonance spectrometry. Anal Chem 70:827–832.

Zako M, Dong J, Goldberger O, Bernfield M, Gallagher JT, Deakin JA. 2003. Syndecan-1 and -4 synthesized simultaneously by mouse mammary gland epithelial cells bear heparan sulfate chains that are apparently structurally indistinguishable. J Biol Chem 278:13561–13569.

Zhang L, Beeler DL, Lawrence R, Lech M, Liu J, Davis JC, Shriver Z, Sasisekharan R, Rosenberg RD. 2001. 6-O-sulfotransferase-1 represents a critical enzyme in the anticoagulant heparan sulfate biosynthetic pathway. J Biol Chem 276:42311–42321.